Analysis of Residual Stress in Surface Overlay of Turbine Rotor by FEM

Kaiyun WANG*, Hao LU*, Yujing JIN*, Fuming GU and Kelin LI*****

*** School of Material Science and Engineering, Shanghai Jiao Tong University, Shanghai 200240, China.**
****Shanghai Institute Special Equipment Inspection & Technical Research, Shanghai 200062, China**
***** Process Research Institute, Sany Truck Crane Machinery Co., LT, Changsha, 410600, China.**

Keywords: Turbine rotor, surface overlay, residual stress, phase transformation

1. Introduction

It well known that residual stress of weld joints can result in many problems to the turbine rotor, such as assembly problems during manufacturing stage and dimensional stability. Seriously, if a crack come into being, the service life of the rotor may be reduced greatly, even, disastrous consequences be brought about，for example, a turbine rotor broke into 20 parts in West Germany the last century just because of cracks being [1]. So, it is essential to study welding induced residual stress for welders and researchers.

Since FEM put forwarded, numerical simulation technology has been developed rapidly. In recent years, its application in weld is becoming more and more widespread, and great progresses have been made. S.W. Wen[2] studied the distribution of residual stress in SAW butt welded bead by FEM. C.H. Lee[3] analyzed the residual stress in high strength steel incorporating solid-state phase transformation.

The present research is undertaken to determine residual stress in surface welded turbine rotor, to analyze their distribution and grasp their evolvement rules. The temperature field and stress field during the welding process are simulated by FEM using a commercial program (ABAQUS). In addition, the welding residual stresses are measured with blind-hole method. After analyzing, the computational results are in accordance with the experimental datum.

2. Experimental procedure

In this study, the blind-hole method was employed to measure the axial and circumferential residual stress in the weld overlay[4]. The detail procedure for measuring the residual stresses on the surface of the specimen (as shown in Fig.1) is as follows: First, attach the two-axis right strain gauges (0°、90°) on the surface of the specimen, here, suppose that the 0°, 90° direction of the strain gauges correspond to the axial direction and circumferential direction of the specimen, respectively. Then, drill a small hole (diameter of 2mm, depth of 2mm) at the specified location on the strain gauges. Residual stresses in the small pieces are released by drilling a hole, axial released strain ε_0, circumferential released strain ε_{90} are measured through static resistance strain gauge and a computer connected with them. Axial residual stress σ_0 and circumferential residual stress σ_{90} can be obtained from the following equations using measured strains:

$$\sigma_0 = \frac{B(\varepsilon_0 + \varepsilon_{90}) + A(\varepsilon_0 - \varepsilon_{90})}{4AB} \quad (1)$$

$$\sigma_{90} = \frac{B(\varepsilon_0 + \varepsilon_{90}) - A(\varepsilon_0 - \varepsilon_{90})}{4AB} \quad (2)$$

where, A, B are axial and circumferential strain released coefficient respectively.

Fig.1 Surface welded specimen

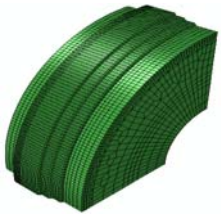

Fig.2 3D FE model

3. FE simulation

Welding process computation can be split into two solution steps: thermal and mechanical analyses. First, the temperature and phase evolution are determined as a function of time in the thermal analysis. Then, the mechanical analysis employs the previous results to get the stresses incorporated with solid-state phase transformation.

3.1 Thermal analysis

As the rotor specimen is axisymmetric, meanwhile, in order to reduce computational time, the FE model is one quarter of the specimen, as shown in Fig.2. During the thermal analysis, the heat input to the weld piece comes from the welding arc, so the double ellipsoidal heat resource model proposed by J. Goldak[5] is employed. Generally, the density, conductivity and specific heat are involved in heat conduction problem. The material of the rotor is 26CrNiMoV10-10, whose density is 7.8e-9 ton/mm^3. Besides, the conductivity and specific heat are temperature-dependent, as indicated in Fig.3. In addition, the latent heat is taken into account during thermal analysis. According to the computational results using JmatPro, the latent heat, solidus and liquidus temperature are 260000mJ*g^{-1}, 1400℃ and 1450℃, respectively.

As for the boundary conditions during the thermal analysis, convection and radiation are both taken into consideration. In order to improve convergence in the FE solution, a constant heat loss coefficient of 0.08mW*m^{-2}*℃$^{-1}$ was assigned to all the free surfaces[2].

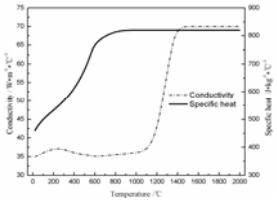

Fig.3 Thermo-physical properties of the material

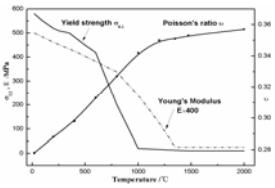

Fig.4 High temperature mechanical properties

3.2 Mechanical analysis

The temperature history solutions obtained from the previous thermal analysis is read into the subsequent mechanical analysis as a thermal loading input. The same FE mesh as in the thermal analysis is employed here. Fig.4 shows the high temperature mechanical properties of the rotor material. Because the base metal and the weldwire are both martensitic steel, meanwhile, the volume will change significantly when autensite transit to martensite, so, the influence of solid-state phase transformation on stresses is taken into account.

In order to compute the martensite fraction in the material during martensitic transformation, the Koistinen-Marbuger relationship expressed by equation (3) is employed here [6].

$$f_M = 1 - \exp(-\alpha(\mathrm{Ms} - \mathrm{T})) \quad (\mathrm{T} \le \mathrm{Ms}) \qquad (3)$$

Where, f_M is martensitic transformation rate; Ms is martensitic transformation initiation temperature, it is 290℃ for the motor material; T is the current temperature during cooling, and α characterizes evolution of the transformation process according to temperature. Generally, for carbon steel, the value of α is 0.045. The differential equation based on Eq.(3) is used in the FE model. Written in the form of increments, the differential equation can be expressed as:

$$\Delta f = -\alpha \cdot \exp(-\alpha(\mathrm{Ms} - \mathrm{T})) \cdot \Delta \mathrm{T} \quad (\mathrm{T} \le \mathrm{Ms}) \qquad (4)$$

Where, ΔT is the temperature increment during cooling. Using above equations, the expansion rate E_{cool} in the course of martensitic transformation can be calculated by following equation [7]:

$$E_{Cool} = f_M \cdot \alpha_M + (1 - f_M) \cdot \alpha_\gamma + \Delta f \cdot \Delta \varepsilon_{M\gamma} \qquad (5)$$

Where, α_M, α_γ are the linear expansion coefficient of full martensite structure and autensite structure, here, they are 1.314×10^{-5}/℃, 2.282×10^{-5}/℃, respectively; $\Delta\varepsilon_{M\gamma}$ is the full volumetric change strain, it is 0.011.

On the other hand, for the inverse transformation behavior during heating, a simplified linear relationship for autensite transformation rate f_γ is adopted [8], expressed as following:

$$f_\gamma = \frac{T - Ac1}{Ac3 - Ac1} \quad (Ac1 < T < Ac3) \qquad (6)$$

Where, Ac1 and Ac3 are the initial and terminate temperature of autensitic transformation, the measured value are 727 ℃ and 809 ℃, respectively. Similarly, the contraction rate E_{heat} in the course of autensite transformation can be calculated by following equation:

$$E_{heat} = (1 - f_\gamma)\alpha_M + f_\gamma \cdot \alpha_\gamma - \Delta\varepsilon_{M\gamma} \cdot (Ac3 - Ac1)^{-1} \cdot \Delta T \qquad (7)$$

4. Results and discussion

Figure 5 shows the thermal cycle at the center point in the weld area during the welding process. The thermal cycle is reported at the first welded joint of the bottom layer. From the figure, it can be observed that the maximum temperature is about 1950℃ or so. This result agrees with the welding process in practice. Further more, it is clear that the inter-pass temperature is well incorporated into the thermal analysis. So, the temperature history solved by thermal analysis is consistent with the expected material behavior.

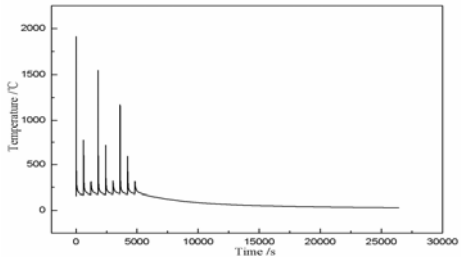

Fig.5 Thermal cycle at the weld area during the welding process

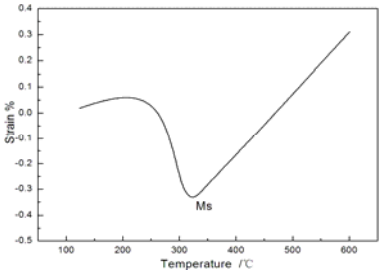

Fig.7 Strain-temperature curve in weld during the course of cooling

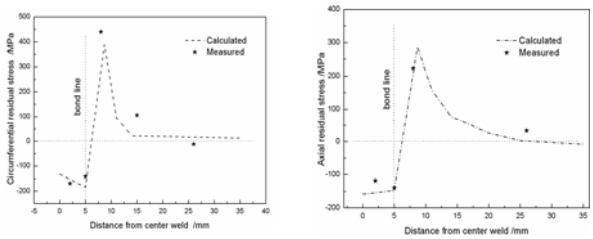

(a) (b)

Fig.6 Distribution of circumferential and axial residual stresses in surface welded rotor

Figure 6 (a), (b) show the circumferential and axial residual stresses calculated by FEM and measured with blind-hole method. The results indicate that the residual stresses calculated by FEM are in accordance with the measured ones. From the figure, it can be concluded that both the circumferential and axial residual stresses are compressive in the weld area. In addition, the residual stresses change from compressive stresses to tensile stresses rapidly in the heat affected zone, and get to its maximum at the area of 5mm far away the bond line, then decrease gradually. The distribution of residual stresses are similar to the results given by Z.Y. Sun[9]. Figure7 shows the change of strain depends on temperature in the weld during the course of cooling. It can be observed that this is a typical martensitic transformation, and the weld metal expands because the specific volume of martensite is bigger than that of austensite. In theory, compressive residual stresses are retained when the temperature decrease to room temperature. And it is confirmed by the measured residual stresses.

5. Conclusion

From the results, it can be concluded that:

1) In the multi-pass welding process, the inter-pass temperature is incorporated into the thermal analysis, affects the material behavior.

2) Circumferential and axial residual stresses are compressive in the weld area. It is helpful to avoid cracks coming into being.

3) Phase transformation during the course of cooling has greatly influence on welding residual stresses. For the martensitic steel whose Ms is lower, compressive residual stresses are obtained, generally.

Acknowledgement

This project is supported by National Natural Science Foundation of China(Grant No:50975176).

References

[1] X.H. Liu, J.T. Lin, Heat Treat. Met. abr. 3(1999).

[2] S.W. Wen, P. Hilton, D.C.J. Farrugia, J. Mater. Process. Tech. 119(2001).

[3] C.H. Lee, K.H. Chang, Comput. Mater. Sci. (2009).

[4] CB 3395-92, Method for residual stress measurement[s] (1992).

[5] J. Goldak, A. Chakravarti, M. Bibby. Metall. Trans. B., 299(1984).

[6] D.P. Koistinen, R.E. Marbuger, Acta Metall. 7(1959) 59-60.

[7] J. Yamamoto, S. Meguro, Y. Muramatsu, N. Hayakawa, K. Hiraoka, Weld. Int. 6(2009) 411-421

[8] D. Deng, Y. Lou, H. Serizawa, M. Shibahara, H. Murakawa, Trans. JWRI 32(2003) 325-333.

[9] Z.Y. Sun, L.X. He, S.H. Cheng, D.D. Sun, Y.R. Wang, Sciencepaper Online.